Journal of Hydrology 416–417 (2012) 28–38

Contents lists available at SciVerse ScienceDirect

Journal of Hydrology

journal homepage: www.elsevier.com/locate/jhydrol

Tidal pumping of water between Bahamian blue holes, aquifers, and the ocean

Jonathan B. Martin *, Jason Gulley [1], Patricia Spellman

Department of Geological Sciences, University of Florida, Gainesville, FL 32611-2120, United States

ARTICLE INFO

Article history:
Received 25 April 2011
Received in revised form 21 October 2011
Accepted 16 November 2011
Available online 25 November 2011
This manuscript was handled by Philippe Baveye, Editor-in-Chief

Keywords:
Blue holes
Cenotes
Bahamas
Carbonate platforms
Tidal pumping
Eogenetic karst

SUMMARY

Exchange of water between conduits and aquifers occurs in many continental karst settings because allogenic recharge from confined catchments causes hydraulic heads in conduits to increase faster than in the aquifer. Most modern carbonate platforms lack allogenic catchments, allowing rainfall to recharge the aquifer uniformly without sufficiently altering head gradients to drive exchange between conduits and aquifers. Some modern carbonate platforms experience tidal variations which could lead to head gradients that drive exchange. To determine the impact of tides on exchange, we measured water elevations at high temporal resolution in the ocean, blue holes and wells on San Salvador Island and Rum Cay, Bahamas. Dampened tidal amplitudes inland indicate diffusivity values (transmissivity/storativity) at wells were around 1.3×10^6 m^2/day and at blue holes were around 76.9×10^6 m^2/day, assuming dampening results only from head loss. These diffusivity values were used to estimate hydraulic conductivity values of around 4.0–294×10^4 m/day although they may be lower if the aquifer thickness is greater than the estimated 10 m. We assume wells provide values representing greater influence of matrix permeability than values from blue holes, which represent a greater influence of conduit permeability. Differences in permeability drive exchange because hydraulic head in the aquifer lags the head in the conduits and blue hole through a tidal cycle. If negligible head loss occurs with flow through conduits, as reflected in lag times less than 10 min, then differences in elevation at the blue holes and the ocean may represent exchange of water between the blue hole and matrix porosity. With this assumption, about 0.9 m^3 of water is exchanged per half tidal cycle, or about 1% of the complete change in volume of water in the blue hole per half tidal cycle. This volume represents an average penetration into the aquifer of 6–8 mm although it could be further in zones with elevated permeability. Exchange is reflected in systematic changes in specific conductivity and pH between high and low tide and the pH changes reflect reaction with the surrounding aquifer material. Since exchange occurs twice daily, cumulative alteration of aquifer porosity could be large. Tidal exchange should decrease away from the coast on large carbonate platforms so that tidally driven alteration will be enhanced at the rims over interior of carbonate platforms.

1. Introduction

Carbonate banks and islands are characterized by complex hydrogeology (e.g., Vacher and Quinn, 1997), which stems from the lack of organized surface drainage, water compositions that vary from fresh to hypersaline, a wide range of water densities, and rapid diagenetic alteration of aquifer rocks. Alteration forms pore volumes that range from microscopic to cavernous and hydraulic conductivities that vary between 10^{-1} and 10^6 m/day and (e.g., Oberdorfer et al., 1990; Whitaker and Smart, 1997b). Young carbonate platforms (referred to as eogenetic karst, Vacher and Mylroie, 2002) may retain primary porosity in the matrix rocks because they have not been fully cemented during burial. In large carbonate platforms subject to wet climates, such as the Yucatan Peninsula, fluxes of fresh water form integrated networks of conduits that efficiently discharge water from the matrix porosity on regional scales (Smart et al., 2006). Cavernous porosity also forms on small platforms that experience drier climates, but this porosity most frequently occurs as isolated macroporous voids (e.g., flank margin caves, Mylroie and Carew, 1990), which only locally influence flow paths within the matrix. Small platforms may also contain zones of elevated permeability that could affect flow, as shown by tidal amplitudes on inland lakes and blue holes, but may be too small to be traversed by humans.

In continental settings, conduits can receive large volumes of allogenic recharge as precipitation drains from catchments formed on confining units. This drainage causes hydraulic heads to increase more rapidly in conduits than in the aquifer and drives water into the aquifer matrix porosity (Martin and Dean, 2001; Moore et al., 2009; Gulley et al., 2011). Gradients reverse during

* Corresponding author. Tel.: +1 352 392 6219.
E-mail address: jbmartin@ufl.edu (J.B. Martin).
[1] Present address: The University of Texas Institute for Geophysics, JJ Pickle Research Campus, Bldg. 196, 10100 Burnet Rd. (R2200), Austin, TX 78758-4445, United States.

0022-1694/$ - see front matter © 2011 Elsevier B.V. All rights reserved.
doi:10.1016/j.jhydrol.2011.11.033

flood recession, allowing water to drain back to the conduits and ultimately to the surface. Modern carbonate platforms commonly lack confining units to focus allogenic water into the aquifers (although see for example, Ayers and Vacher, 1986; Vacher and Mylroie, 2002), and recharge generally flows directly and diffusely to the aquifer. Because recharge is uniformly distributed, allogenic recharge cannot increase hydraulic head in conduits faster than heads in the matrix porosity to drive exchange. Consequently, little work has been done to estimate the exchange of water between conduits, zones of elevated permeability, and matrix porosity on carbonate platforms. Carbonate platforms experience tidal fluctuations, which decrease with distance from the ocean, but could be sufficiently large to drive exchange (e.g., Ferris, 1951; Townley, 1995). Head differences between the ocean, conduits, and matrix porosity may establish gradients that could facilitate exchange between conduits and matrix. Since tidally driven exchange would occur once or twice per day, its cumulative effects might be capable of extensive exchange between the conduits and matrix porosity with associated influence over diagenetic alteration of the platforms.

The exchange of water between conduits or other higher permeability zones and the aquifer matrix has important implications for the diagenetic alteration of aquifers through cementation and dissolution. Dissolution of unstable minerals such as aragonite can drive precipitation of more stable minerals such as calcite, thereby redistributing solid phase material, and creating macropores while retaining the bulk porosity (e.g., Budd, 1988). Cementation can form confining layers with reduced permeability compared to the remainder of the aquifer (Ayers and Vacher, 1986; Vacher and Mylroie, 2002). Dissolution results when the recharged water is undersaturated with respect to carbonate minerals (e.g., Moore et al., 2010), for example when organic matter is oxidized by microbes using dissolved oxygen or sulfate to produce carbonic and sulfuric acids (e.g., Bottrell et al., 1990; Stoessell et al., 2002; Whitaker and Smart, 2007a, 2007b; Moore, 2009; McGee et al., 2010). Undersaturation also may result from mixing of water with different chemical compositions (mixing corrosion, e.g., Runnells, 1969; Wigley and Plummer, 1976; Mylroie and Carew, 1995), though the importance of mixing corrosion has been questioned (e.g., Whitaker and Smart, 1997b; Melim et al., 2002; Moore et al., 2010). Mixing corrosion may be focused at tops and bottoms of fresh water lenses, where vadose infiltration mixes with lens water and lens water mixes with underlying saltwater, respectively (Cant and Weech, 1986). Dispersion between salt and fresh water forms a halocline of variable thickness, which depends on the size of islands and permeability of aquifer rocks (Whitaker and Smart, 1997b). Tidal pumping may expand mixing zones as well as increase dispersion of undersaturated water resulting from oxidation of organic matter.

Water-filled vertical depressions, which are referred to as blue holes or black holes in the Bahamas and cenotes in the Yucatan Peninsula, form by dissolution and/or conduit collapse (Mylroie et al., 1995; Perry et al., 1995; Schwabe and Herbert, 2004). Many blue holes are density stratified and particulate organic carbon accumulates at the density interface (Bottrell et al., 1990; Stoessell et al., 2002), which when oxidized could dissolve aquifer rocks if water exchanges between the blue hole and aquifer. Exchange of water occurs between blue holes and the matrix along a bank margin fracture along the coast of Andros Island, Bahamas (Stringfield and LeGrand, 1971; Whitaker and Smart, 1997a). These conduits reverse flow through a tidal cycle, resulting in the discharge of fresh water to the ocean during ebbing tides and inflow of saltwater to the aquifer during flooding tides. Based on lags in tidal cycles between the blue holes and the ocean, mixed water was estimated to be injected into the aquifer a distance of up to 200 m around the fracture system creating a halo of diagenetically altered rock (Whitaker and Smart, 1997a).

Profiles of chemical composition in the water column of blue holes and cenotes have been used previously to estimate water–rock reactions and hydraulic parameters (e.g., Stoessell, 1995; Whitaker and Smart, 1997a; Beddows et al., 2007) and variations in head resulting from tidal fluctuations have been used to estimate hydraulic parameters (e.g., Stringfield and LeGrand, 1971). No geochemical observations have been conducted at tidal time scales or made sequentially through numerous tidal cycles. In this paper, we present measurements of water levels and limited chemical data (specific conductivity, dissolved oxygen concentrations, and pH) that were collected at high spatial and temporal resolution over several tidal cycles from blue holes on San Salvador Island and Rum Cay, Bahamas using logging environmental sensors. The data provide estimates of aquifer properties, provide constraints on how tidal pumping affects exchange between the ocean, blue holes, and the aquifer, and reflect diagenetic alteration of the aquifer rocks.

2. Field areas

San Salvador Island and Rum Cay are located in the southeastern Bahamas on two small individual carbonate platforms, which are covered almost entirely by the islands (Fig. 1). Both islands have numerous outcrops and multiple water-filled blue holes and lakes. The exposed rocks on both islands fit the stratigraphy proposed by Carew and Mylroie (1995). This stratigraphy splits the originally defined Lucayan Limestone (Beach and Ginsburg, 1980) into three separate formations: the Holocene Rice Bay Formation, the Pleistocene Grotto Beach (Marine Isotope Stage (MIS) 5e) and Owl's Hole (pre-MIS5e) formations. These formations are separated by terra rossa paleosols that were deposited when the tops of the platforms were exposed during interglacial times. Exposure led to dissolution and reprecipitation of the original detrital carbonate minerals during the conversion from aragonite to calcite, with an associated increase in the bulk permeability of the rock (e.g., Vacher, 1988; Vacher and Wallis, 1992). San Salvador Island and Rum Cay contain numerous flank margin caves that formed during MIS5e and do not greatly influence groundwater flow (e.g., Mylroie and Carew, 1990). Tidal fluctuations in lakes and blue holes in the interior of the islands suggest there may be conduit connections with the ocean (Davis and Johnson, 1989).

The two islands are separated by about 30 km and, despite sharing similar climates, have differing amounts of surface water. More than half of the surface of San Salvador Island is covered by hypersaline lakes in swales between dune ridges. The dunes contain fresh water lenses that drain to the lakes (Davis and Johnson, 1989). In contrast, few dunes occur on Rum Cay, and consequently, it contains few lakes (Fig. 1). Geomorphologic differences between the two islands could result from their orientations (Martin and Gulley, 2010). The main axis of San Salvador is oriented north–south, perpendicular to the trade winds, which allowed development of dunes and associated lakes. In contrast, Rum Cay is oriented parallel to the trade winds and thus dunes are found only along the northeastern and southwestern coasts. Most of the interior of Rum Cay was classified as being deposited in a large tidal creek system during MIS5e (Mitchell, 1987). This tidal creek system resulted in flat topography throughout the interior of the island, which is now slightly above sea level (Fig. 1). Surface water is confined mostly to small (1–2 m diameter) dissolution features that intersect the groundwater table, although a few larger (tens of m) blue holes are present.

3. Methods

Data were collected during two sampling trips, one to both San Salvador Island and Rum Cay between April 22 and May 1, 2010 and the other to San Salvador Island between June 15 and June

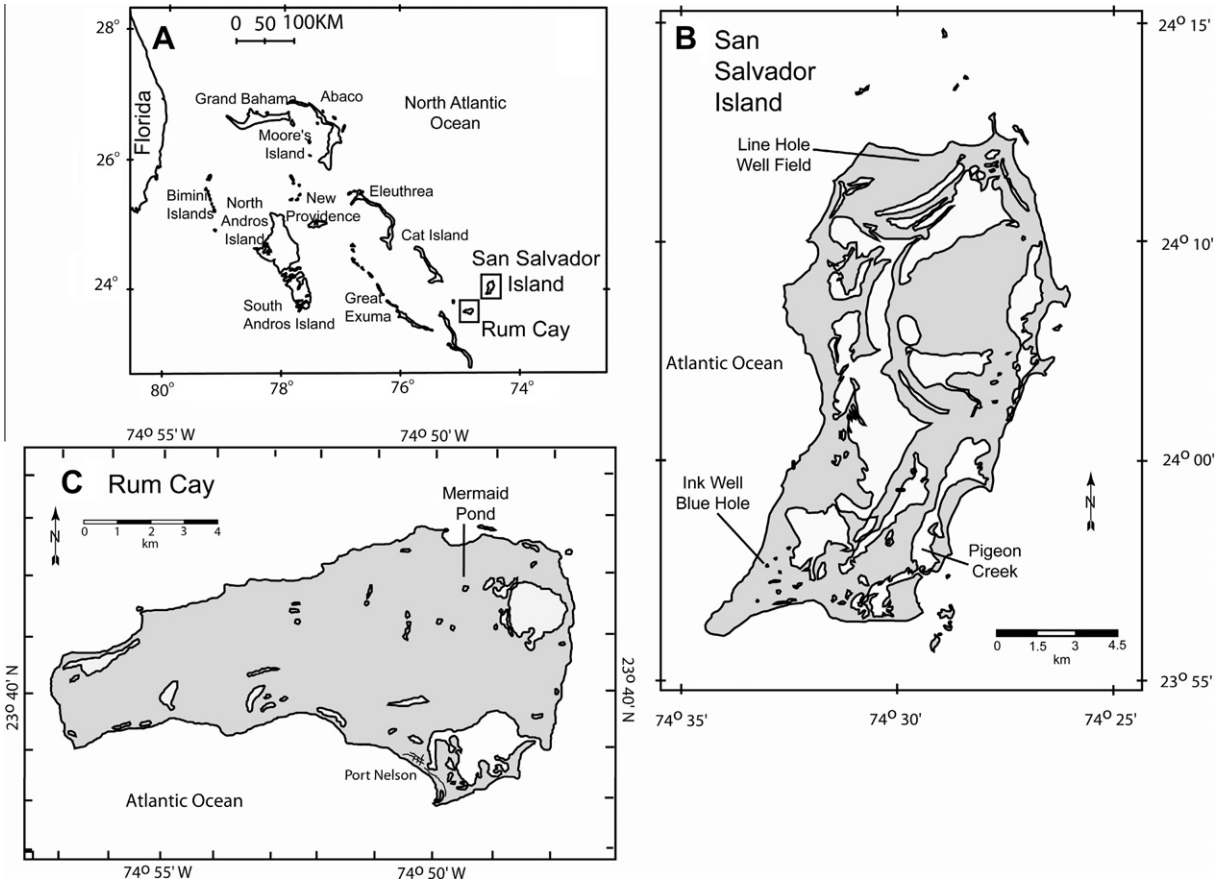

Fig. 1. Location maps of (A) San Salvador Island and Rum Cay, Bahamas, (B) San Salvador Island, and (C) Rum Cay. The dark gray area represents land and the light gray area represents surface water, including hypersaline lakes, and marine and fresh water blue holes.

21, 2010. During these trips, water levels were measured at high temporal resolution in Ink Well Blue Hole in southeastern San Salvador Island (Fig. 1B), and in Mermaid Pond approximately in the center of Rum Cay (Fig. 1C), along with selected chemical parameters (specific conductivity, dissolved oxygen (DO), and pH). Line Hole well field near the northern coast of San Salvador Island was sampled during both trips and chemical loggers were left in two wells between the trips. During the second trip, tidal elevations were measured at high resolution near the mouth of Pigeon Creek, a large saline lake on San Salvador open to the ocean.

3.1. Measurements of water elevations, DO concentrations, and pH

Time series measurements of conductivity, temperature and depth were made at four depths in Ink Well Blue Hole (approximately 60, 200, 400 and 600 cm depth below the water surface) and at approximately 30 cm below the water surface in Pigeon Creek from June 16 to 20, 2010. These measurements were made with In Situ AquaTroll 200 logging instruments at a rate of one sample every 10 min. The fixed depth sampling in Ink Well Blue Hole was accomplished by hanging the AquaTrolls from a nylon line strung tightly across the surface of the blue hole. The time series data from Pigeon Creek are used to observe tidal amplitude and periodicity for the ocean and at the other locations to observe tidal amplitude and periodicity at inland sites on the carbonate platforms. Because our measurements of ocean tides are limited to 4 days at Pigeon Creek, we supplement tidal data for our other sampling periods using the XTide Tide Prediction Server (http://www.mobilegeographics.com:81/locations/5570.html). Conductivity, temperature, and depth were also measured in two wells from Line Hole well field from April 25 to June 16, 2010 at a rate of one sample every 20 min. Line Hole well field consists of 13 wells oriented perpendicular to the northern coast of San Salvador Island that cross a shore-parallel dune. The sampled wells are the 8th and 10th wells away from the ocean and are referred to here as well 8 and well 10. They are located 24° 06.794′N, 74° 29.320′W and 24° 06.763′N, 74° 29.339′W, respectively.

Vertical profiles of specific conductivity, temperature and depth (CTD) were measured through the water column at Ink Well Blue Hole and Mermaid Pond using an In Situ AquaTroll 200 logging instrument (Table 1). Most profiles were measured at or within a couple hours of high or low tide, except for the profiles measured on April 25 and June 17 at Ink Well Blue Hole, which were made on a flooding tide halfway between low and high tide. Except for the measurements made on April 22 and 23 at Ink Well Blue Hole, each profile was measured at sequential tidal extremes. The high tide

Table 1
Location of vertical profiles through blue holes.

Location	Date	Tidal stage[a]	Parameters[b]
Inkwell	April 22, 2010	At HT	D, SpC
Inkwell	April 23, 2010	At LT	D, SpC
Inkwell	April 25, 2010	2 h after LT	D, SpC
Inkwell	April 25, 2010	Intermediate, rising tide	D, SpC
Inkwell	June 17, 2010	Intermediate, rising tide	D, SpC, DO, pH
Inkwell	June 17, 2010	1.5 h after HT	D, SpC, DO, pH
Mermaid Pond	April 28, 2010	2.5 h after HT	D, SpC
Mermaid Pond	April 28, 2010	1 h after LT	D, SpC

[a] HT = high tide; LT = low tide.
[b] D = depth, SpC = specific conductivity, DO = dissolved oxygen concentrations.

profile measured on April 22 was separated by intervening low and high tides before the low tide profile was measured on April 23 (Table 1). The profiles were measured from a raft floated to approximately the center of the blue holes. No bathymetric maps are available of the blue holes, but several soundings were made in an attempt to locate their greatest depth. During the April 2010 sampling time, the raft was not attached to shore and its position was maintained by paddling the water. These samples may have variations within and between profiles caused by lateral motion of the raft. During the June sampling, the raft was attached to the nylon line used to hang the AquaTrolls and thus both profiles were collected at identical locations in the blue hole.

Profiles were measured by manually lowering the AquaTrolls through the water column. The sampling rate was set to one measurement per minute, which is their fastest logging rate. Measurements were made at increments of approximately 30 cm during the April sampling trip and approximately 20 cm during the June sampling trip, although plotted depths are derived from the logger data. The loggers were held at each depth for 1 min to ensure equilibration of the instrument with the ambient characteristics. Depth profiles of DO concentrations and pH were measured at Ink Well Blue Hole at high and low tide using an YSI model 6920 logging instrument with an attached Schlumberger CTD-diver used to measure depth. The sampling rate was 10 s, the depth increments were approximately 20 cm, and measurements were for 1–2 min at each depth. All values were averaged at each depth, but there was little difference within each depth interval indicating that equilibration from one depth to the next is rapid. Depth was measured relative to the water surface, profiles were corrected to an arbitrary benchmark 1 m above mean low low water (MLLW).

3.2. Estimates of aquifer diffusivity

Aquifer diffusivity, the ratio of aquifer transmissivity to aquifer storage coefficient, can be estimated through comparison of the lag in tidal phase, L, described by

$$L = R_\theta - F_\theta \tag{1}$$

where R_θ is the phase of the tidal response in the inland site, for example a well or blue hole and F_θ is the phase of the forcing at the tidal boundary, for example the shoreline. Aquifer diffusivity can also be derived from the decrease in the amplitude of the tidal height, which is described by the tidal efficiency, E, defined by

$$E = \frac{R_a}{F_a} \tag{2}$$

where F_a is the amplitude of the forcing at the tidal boundary, for example the shoreline, and R_a is the response at the inland site, for example a well or blue hole (Ferris, 1951; Townley, 1995). The governing equation for 1D transient groundwater flow with tidal boundary conditions is

$$\frac{\partial^2 h}{\partial x^2} = \frac{S}{T}\frac{\partial h}{\partial t} \tag{3a}$$

with boundary condition

$$h(0,t) = H_a \cos(\omega t - H_\theta) \tag{3b}$$

where x is the horizontal distance from the shoreline to the inland location, S is aquifer storage coefficient, T is the aquifer transmissivity, h is the water elevation, t is time, H_a is the amplitude of the tidal fluctuation at the shoreline, ω is the tidal frequency and H_θ is the phase measured in radians. An analytical solution to Eq. (3) provides expressions for E and L (Ferris, 1951; Townley, 1995)

$$E = e^{-x\sqrt{\frac{\omega S}{2T}}} \tag{4a}$$

$$L = x\sqrt{\frac{SP}{4\pi T}} \tag{4 b}$$

where P is the tidal period, which for these islands is about 0.52 days. These solutions can be rearranged into expressions for aquifer diffusivity in terms of the tidal efficiency and lag:

$$\frac{T}{S} = \frac{\pi x^2}{(\ln E)^2 P} \tag{5a}$$

$$\frac{T}{S} = \frac{x^2 P}{4\pi L^2} \tag{5 b}$$

We use these equations below to estimate the aquifer diffusivity based on measured tidal data at the blue holes, wells and the ocean.

4. Results

4.1. Tidal variations

We assess the compatibility of the two sources of tidal data by comparing the time from high and low tides measured in Pigeon Creek to the time of the corresponding high and low tide provided by the XTide Tide Prediction Server (Fig. 2). Times are consistent between the two measurements over the seven tidal cycles that we measured at Pigeon Creek, indicating that these data may be used interchangeably. The average difference for the time of the high and low tides for the two measurements is about 20 min, with a standard deviation of about 17 min.

Ink Well Blue Hole shows tidal periodicity in both its water level and the specific conductivity of water at fixed depths within water column from about 1500 h on June 16, 2010 through around 1400 h on June 20, 2010 (Fig. 3). The amplitude and periodicity of the tidal variations at Ink Well Blue Hole appear similar to the amplitude and periodicity of tidal variations at Pigeon Creek (Fig. 3B). This inference is supported by cross correlations of the tidal frequencies at Pigeon Creek and Ink Well Blue Hole, which show that tidal frequencies are identical within a 10 min lag at the blue hole and Pigeon Creek (Fig. 4). This lag is smaller than the sampling rate used to measure the water elevations at the two locations.

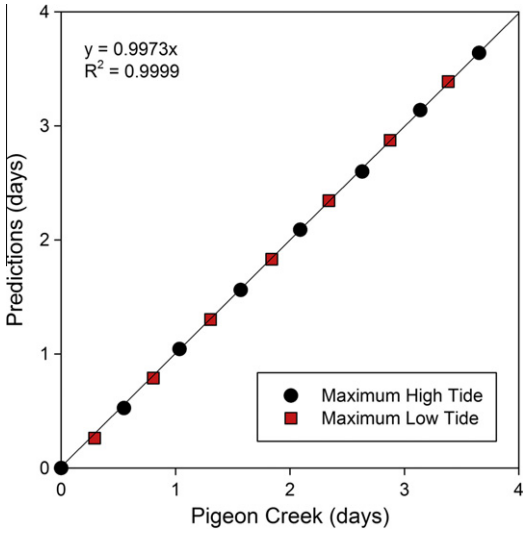

Fig. 2. Comparison of frequency of tides measured in Pigeon Creek with tides predicted from XTide Tide Prediction Server. Points represent the time (days) since the first low tide measured in Pigeon Creek.

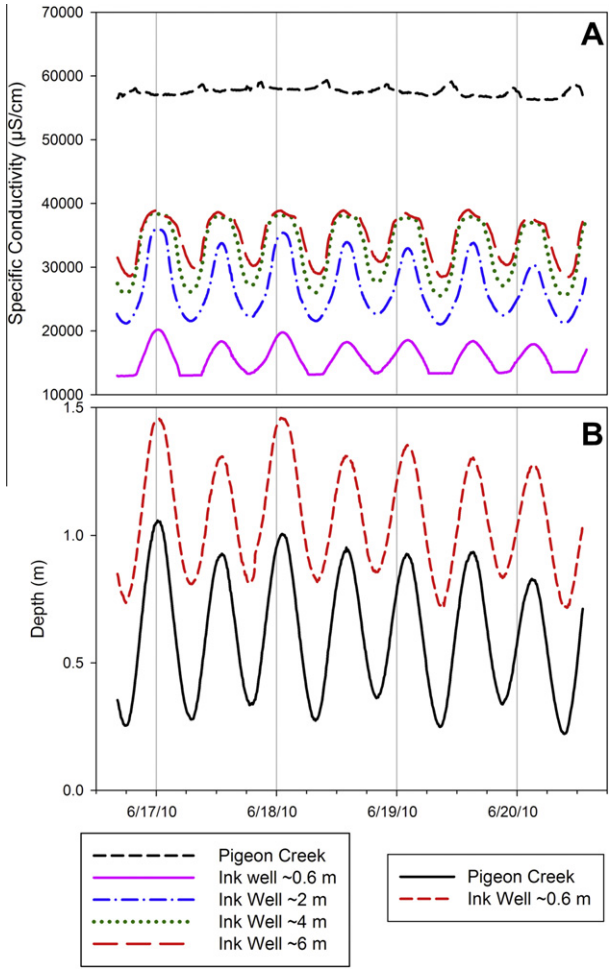

Fig. 3. (A) An approximately 4-day long time series of variations in specific conductivity at four depths within Ink Well Blue Hole and at Pigeon Creek. Legend on left and (B) variations in water level at Ink Well Blue Hole and Pigeon Creek over the same time period as in panel A. The absolute depths are arbitrary but plotted so that the greatest depth represents high tide. Legend on right.

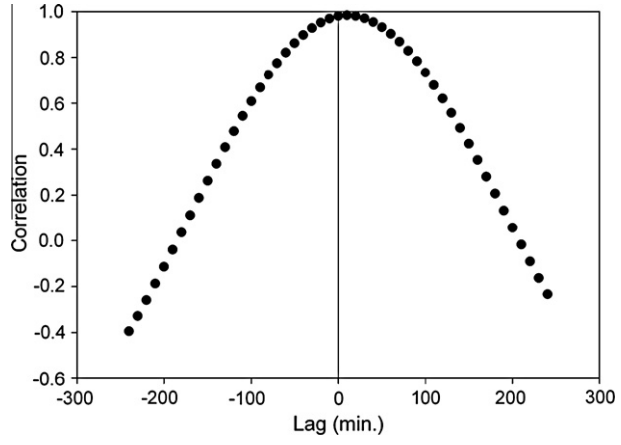

Fig. 4. Cross correlogram for correlations between tidal frequency at Pigeon Creek and Ink Well Blue Hole.

The specific conductivity at Pigeon Creek shows small variations ranging around 56,000 µS/cm to 59,000 µS/cm (Fig. 3A). The maximum specific conductivity occurs as short-lived peaks corresponding to maximum low tide. These small peaks may reflect flushing of high salinity water that had been concentrated through evaporation in Pigeon Creek. Specific conductivity at Ink Well Blue Hole also shows tidal periodicity, but the amplitude of the change in specific conductivity varies with the depth of the loggers (Fig. 3A). For example, specific conductivity of the logger about 6 m below the surface exhibits an amplitude of about 10,000 µS/cm, but the logger about 0.6 m below the surface exhibits an amplitude of about 6,000 µS/cm. The largest amplitude, of about 15,000 µS/cm, occurs at the logger about 2 m below the surface. At all depths, the highest values of specific conductivity occur at high tide and the lowest values of specific conductivity occur at low tide. At depths approximately 2 m below the surface, specific conductivity varies through time as a smooth sinusoid, but at 4 and 6 m below the surface, the maximum conductivity values exhibit a flattening of the smoothly varying values immediately following high tide. Similarly, the logger at approximately 0.6 m below the surface exhibits constant specific conductivity values of around 13,000 µS/cm during the maximum low tides. These constant values occur only every other low tide, corresponding to the largest tidal range between low tide and the preceding high tide (Fig. 3).

4.2. Chemical depth profiles

Depth profiles of specific conductivity show haloclines that have variable gradients and thicknesses at different times in the tidal cycles at Ink Well Blue Hole and Mermaid Pond (Fig. 5). The gradients of the haloclines also vary over the 2 months separating the two primary sampling times at Ink Well Blue Hole. In April 2010, the freshest water at Ink Well Blue Hole had a specific conductivity of around 7500 µS/cm regardless of the tidal elevation, but the specific conductivity increased immediately below the surface to the saltiest water at the base of the profile, which had specific conductivity values that varied from about 27,000 µS/cm at low tide on April 23 to around 36,000 µS/cm at high tide on April 22 as well as approximately 2 h after high tide on April 25. The profile from April 25, which was measured on a flooding tide half way between low and high tide, shows specific conductivity values of around 33,000 µS/cm at the base, slightly lower than the specific conductivity value at a similar depth at high tide. In the upper portion of the halocline, specific conductivity values are similar to those measured during low tide (Fig. 5A).

In June 2010, the lowest salinity water at the surface of Ink Well Blue Hole exhibited specific conductivity values of around 13,000 µS/cm (Fig. 5B). This value represents an increase of around 5500 µS/cm over the lowest salinity found during the April sampling. Similar to the April sampling time, specific conductivity of the low-salinity water remained constant regardless of the time within the tidal cycle it was measured. Rather than immediately increasing salinity from the surface as during the April sampling, however, the low-salinity layer showed constant values with depths that ranged from about 85 cm during sampling soon after high tide to around 40 cm for the sampling period intermediate between high and low tide (Fig. 5B). Specific conductivity at the base of the low tide profiles is similar during sampling at low tide and sampling during the rising tide. At both times, the specific conductivity was about 35,000 µS/cm for the low tide profile and 37,500 µS/cm for the intermediate tide profile. These values are also similar to the value found at high tide in the April sampling period (Fig. 5A). Although the two profiles measured in June reach approximately the same depth, the layer of saline water at the base of the halocline was thicker during the intermediate tide than during low tide sampling. The values of specific conductivity were lower at all depths within the halocline when measured during intermediate tide than when measured at high tide.

Only minor differences occur in the profiles of specific conductivity measured near high and low tide at Mermaid Pond, but the differences are consistent with differences found at Ink Well Blue

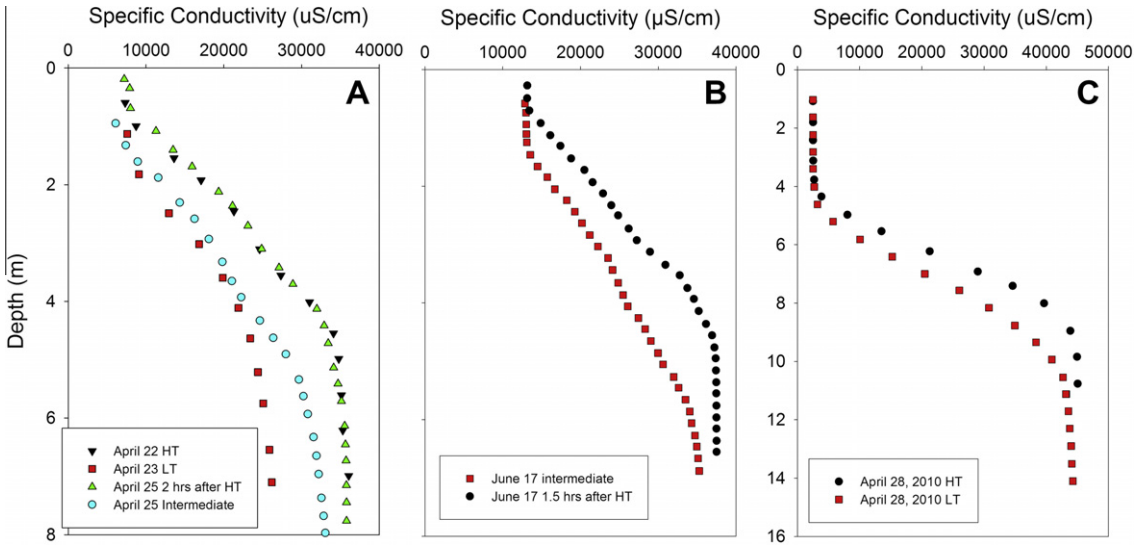

Fig. 5. Depth profiles of specific conductivity measured at Ink Well Blue Hole in (A) April 2010, (B) June 2010, and (C) Mermaid Pond in April 2010. The datum for the profiles is an arbitrary point 1 m above the mean low low water (MLLW).

Hole (Fig. 5C). The upper fresh water layer has a constant value of around 2500 µS/cm at both high and low tide, but is about 30 cm thicker at low tide, when the thickness was about 2.8 m compared with high tide when the thickness was about 2.5 m. Specific conductivity in the saline water at the base of the profiles is similar at both high and low tide with values around 45,000 µS/cm, but the top of the saline water is about 9.9 m below the surface during the low tide sampling but only about 8.3 m at high tide sampling, or about 1.6 m shallower at high than at low tide. The change in the elevation of the saline layer increased the gradient of the halocline from about 6000 µS/cm per m at low tide to 7300 µS/cm per m at high tide. The steeper gradient causes all values of specific conductivity to be lower when measured at low than at high tide.

At Ink Well Blue Hole in June 2010, both pH and DO concentrations decrease rapidly with depth to approximately 1 m below the top of the halocline at a total depth of around 2 m (Fig. 6). Below that depth the DO concentrations remain constant at approximately 0.1 mg/L regardless of when the tidal cycle was sampled. The pH profile measured 1.5 h after high tide shows a constant increase of 0.06 pH units from 7.11 to 7.17 from about 2 m below the surface to the base of the profile. The profile collected between low and high tide differs and shows a sharp increase near the middle of the halocline from 7.14 to 7.22 at a depth of around 4 m below the surface.

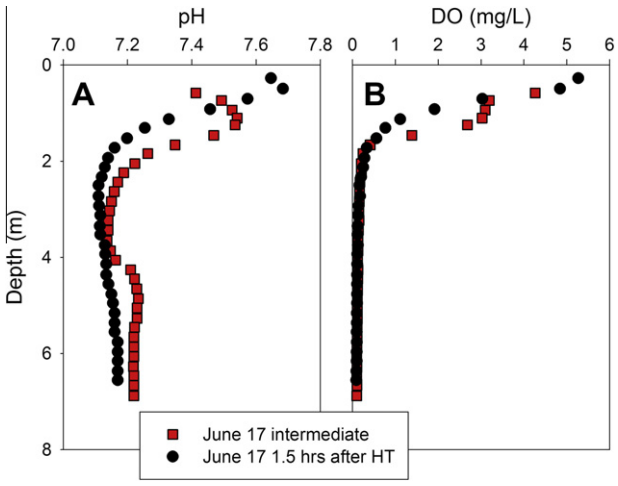

Fig. 6. A. pH and **B.** dissolved oxygen concentrations versus depth in Ink Well Blue Hole on a flood tide intermediate between low and high water and 1.5 h after high tide. The datum for the profiles is an arbitrary point 1 m above MLLW.

4.3. Aquifer properties

Aquifer diffusivity was estimated across the islands using Eq. (5a) and measured tidal efficiencies between the coast, Ink Well Blue Hole, Mermaid Pond, and wells 8 and 10 from Line Hole well field. Aquifer diffusivity could not be estimated with Eq. (5b) because the lag between the coast, blue holes and wells was less than the sampling time (e.g., Fig. 4). Data were available for tidal amplitudes at wells 8 and 10 over several months and thus diffusivity was estimated using Eq. (5a) for each well on the basis of tidal elevation over 3 days of spring tide and 4 days of neap tides. Well 10 is characterized by diffusivity values that are about 1.7 times greater than well 8, with diffusivity ranging from 1.3 to 3.0×10^6 m^2/day. The differences between spring and neap tides were 0.4×10^6 and 0.8×10^6 m^2/day for well 8 and well 10, respectively (Table 2). Water elevation data are available from Ink Well Blue Hole for a 5 day period during a neap tide and at Mermaid Pond for a 4 day period of spring tide. We do not have the alternating spring and neap tide data for these sites and thus cannot determine effects of bi-weekly changes in tidal amplitude on diffusivity. Diffusivity was estimated to be greater at Ink Well Blue Hole (76.9×10^6 m^2/day) than at Mermaid Pond (52.6×10^6 m^2/day). These values are about 15–75 times greater than the diffusivity at the wells.

Transmissivity and hydraulic conductivity values can be estimated from the diffusivity values assuming values for storativity and aquifer thickness. Whitaker and Smart (1997a) use storativity values of 0.3 to estimate hydraulic conductivity for pump tests of wells around the Bahamas, and we use the same value here to estimate transmissivity. We assume the aquifer is the zone in which horizontal flow occurs between the ocean and the blue holes and wells. Although the fresh water lens is only a few tens of centimeters thick at Ink Well Blue Hole and several meters thick at Mermaid Pond, the halocline extends to several meters depth at both locations, suggesting lateral flow may occur to at least this depth. Fresh water lenses are around 8–10 m at two deep wells at Line Hole well field. Estimates of flow to depths of a few tens of meters were made based on Sr isotope ratios in water collected

Table 2
Estimates of hydraulic diffusivity and hydraulic conductivity.

Dates	Location	Distance (m)	Tidal amplitude (Fa) (m)	Aquifer amplitude (Ra) (m)	Tidal efficiency (E) (-)	Hydraulic diffusivity (T/S) (m^2/day)	Hydraulic conductivity (K)[a] (m/day)
6/16 – 6/20	Ink Well	550	0.21	0.18	0.87	76.9×10^6	294×10^4
4/27 – 4/29	Mermaid Pond	1100	0.45	0.31	0.69	52.6×10^6	158×10^4
4/26 – 4/29	Well 8 (spring)	404	0.45	0.21	0.45	1.7×10^6	5.1×10^4
5/7 – 5/11	Well 8 (neap)	404	0.26	0.11	0.44	1.3×10^6	4.0×10^4
4/26 – 4/29	Well 10 (spring)	470	0.45	0.23	0.50	3.0×10^6	8.9×10^4
5/7 – 5/11	Well 10 (neap)	470	0.26	0.12	0.48	2.2×10^6	6.7×10^4

[a] Assuming $S = 0.3$ (Whitaker and Smart, 1997a) and an aquifer thickness of 10 m.

from around San Salvador Island and Long Island (Martin and Moore, 2008). We thus assume an aquifer thickness of 10 m to estimate hydraulic conductivity values from the estimated diffusivity values. With these assumptions, the hydraulic conductivity based on diffusivity at wells 8 and 10 ranges from 4.0 to 8.9×10^4 m/day (Table 2). Estimates of hydraulic conductivity are about 20–70 times greater at the blue holes, ranging from 158×10^4 m/day at Mermaid Pond to 294×10^4 m/day at Ink Well Blue Hole. Eq. (1) assumes that the variation in the thickness of the aquifer with tides is small relative to the total thickness of the aquifer (Townley, 1995). Assuming an aquifer thickness of 10 m and tidal variations of between 0.11 and 0.31 m, the change in the thickness of the aquifer varies by around 1–3% and should be sufficiently small to satisfy the assumption of small changes in aquifer thickness. Because the thickness of the aquifer is unknown, absolute values of hydraulic conductivity may be incorrect, but they demonstrate hydraulic conductivity calculated from well data is orders of magnitude less than calculations based on data from the blue holes.

5. Discussion

In the following discussion, we estimate aquifer hydraulic properties based on the observed changes in water elevation in the ocean, wells and blue holes. These estimates suggest that higher conduit than matrix permeability drives exchange between matrix porosity, conduits, and blue holes and is responsible for the changes in the chemical depth profiles observed in the blue holes.

5.1. Estimates of aquifer properties

Estimates of hydraulic conductivity are scale dependent in karstic aquifers. Laboratory tests at length scales of centimeters yield values that can be more than eight orders of magnitude smaller than estimates made in the field over lengths of tens of kilometers (e.g., Whitaker and Smart, 1997b; Ford and Williams, 2007). On San Salvador Island and Rum Cay, tidal amplitudes were dampened only slightly between the ocean and Ink Well Blue Hole, Mermaid Pond, and wells 8 and 10 at Line Hole well field. Even with the slight dampening of tidal amplitudes, the blue holes show diffusivity values that are 20–60 times greater than the wells (Table 2). The land surface shows evidence for a terra rossa paleosol at Ink Well Blue Hole, Mermaid Pond, and Line Hole well field, indicating that the wells and blue holes are within the Grotto Beach Formation. This formation has enhanced permeability caused by dissolution and development of preferential flow paths because of its greater age than the overlying Rice Bay Formation (e.g., Vacher, 1988). The Grotto Beach Formation should thus dominate exchange between the ocean and blue hole. Assuming bulk storativity for the Grotto Beach Formation is constant at all of our sampling sites, transmissivity of the aquifer at the blue holes would be 20–60 times higher than transmissivity of the wells. The difference in estimated transmissivity may reflect differences in the permeability of the sampled portion of the aquifer at each site. In wells 8 and 10, the depth of water is about 2.5 m while at Ink Well Blue Hole and Mermaid Pond, the depth of water is about 7 and 14 m respectively. The blue holes are thus more likely to encounter highly transmissive zones because of their larger wetted surface area than the wells. In addition, blue holes commonly have openings at their base suggesting they are linked to conduits, possibly representing collapse (Davis and Johnson, 1989). Blue holes may thus provide representative values of transmissivity for conduits, while wells may provide representative values of aquifer matrix rocks.

Our lowest estimates of hydraulic conductivity, of around 5×10^4 m/day at Line Hole well field (Table 2), are similar to the highest values for wells found in Little et al. (1973, reported in Whitaker and Smart, 1997). Our highest estimate of hydraulic conductivity of 294×10^4 m/day, at Ink Well Blue Hole, is a couple orders of magnitude higher than Little's (1973) values. These high values suggest that our estimate of aquifer thickness may be too low; an aquifer thickness greater than our estimate of 10 m would reduce the hydraulic conductivity values to those similar to Little et al. (1973). Little's (1973) estimates were based on tidal lags in wells penetrating the Grotto Beach Formation (reported as Lucayan Limestone) on North Andros Island. Since values of hydraulic conductivity in karst systems are highly scale dependent (e.g., Ford and Williams, 2007) our highest values are likely to represent hydraulic conductivity of high permeability zones intersected or created by the blue hole. The values found in the wells also indicate zones of elevated hydraulic conductivity, but the fact that they are 40–75 times less than those in the blue hole also indicate an influence from the matrix. Regardless of the absolute values of estimated hydraulic conductivity, the range of hydraulic conductivity over several orders of magnitude may create hydraulic gradients sufficient to exchange water between conduits and aquifer matrix, if tides can cause head to increase in high permeability zones faster and to higher values than in the matrix.

5.2. Estimate of magnitude of exchange between blue holes and aquifer

The low topographic relief of San Salvador Island and Rum Cay and their high matrix hydraulic conductivities indicate that the water table elevation should primarily be a function of ocean tidal fluctuations. The tidal changes will alter head gradients between the ocean and a monitoring site such as Ink Well Blue Hole. These head gradients, H, can be estimated based on the difference between the measured and average elevation of water levels at the ocean (as measured in Pigeon Creek) and at Ink Well Blue Hole according to

$$H = [(E_{IWm} - E_{IWa}) - (E_{Om} - E_{Oa})]/x \quad (6)$$

where E_{IWm} and E_{IWa} are the measured and average water elevation of Ink Well Blue Hole, E_{Om} and E_{Oa} are the measured and average elevation of the ocean as measured in Pigeon Creek, and x is 550 m, the distance between the coast and Ink Well Blue Hole (Fig. 7). Because we do not have absolute elevation measurements,

Eq. (6) assumes that the average elevation at Ink Well Blue Hole is identical to the average elevation at the ocean. The head gradients estimated using this technique are thus minimum if the water table at any point between Ink Well Blue Hole and the ocean is elevated from recharge of precipitation. San Salvador Island and Rum Cay have annual average excess potential evaporation over precipitation (Sealey, 2006), suggesting the water table will be low and unlikely to exceed the average water table elevation during tidal cycles. Assuming a Ghyben–Herzberg relationship and a thickness of the fresh water lens of about 1 m (Fig. 5), the elevation of the water table would be around 2.5 cm or about 3% of the tidal range. Eq. (6) indicates head gradients are small with a maximum gradient of around 2×10^{-4}. The gradients are oriented inland during high tide and offshore during low tide, and thus the gradients will be zero approximately midway through the tidal cycle (Fig. 7).

If tidal flow into and out of Ink Well Blue Hole was idealized as occurring through a conduit without any head loss, the tidal amplitude of the blue hole and ocean would be identical and there would be no lag. If no head loss occurs during flow through the conduits, however, estimates of aquifer diffusivity made using Eq. (5a) would be invalid. Some head loss must occur, but it is likely to be small considering the measured tidal lag is less than 10 min between the ocean and the blue hole (Fig. 4). Regardless of the small lag, the tidal amplitude of Ink Well Blue Hole is less than the ocean tidal amplitude by around 13% (Table 2). Exchange of water between Ink Well Blue Hole and the matrix porosity may be caused by differences in the rate that hydraulic heads in the aquifer matrix, blue hole and ocean respond to tidal forcing (Fig. 8). During an ebb tide, water flows from the blue hole more rapidly than from the matrix. As a result, head is higher in the matrix than in the blue hole, and water flows from the matrix to the blue hole (Fig. 8A). During a flood tide, the efficient hydraulic connection between the blue hole and the ocean causes the elevation of water in the blue hole to rise more rapidly than in the matrix causing water to flow from the blue hole into the matrix (Fig. 8B).

Using the conceptual model presented in Fig. 8, we can estimate the amount of water exchanged between the blue hole and the matrix porosity (Table 3 and Fig. 7). The area of the surface of blue hole times the vertical change in water level between high and low tide estimates the change in the tidal volume of Ink Well Blue Hole. Assuming no head loss so that the elevation of the blue hole and ocean should be equal, the volume of water exchanged with the matrix porosity can be estimated by subtracting the elevation of water in the blue hole from the elevation of the ocean. The elevation was measured at 10 min increments and these values were calculated for each increment and then summed over each half tidal cycle to estimate the total volume of water lost to or gained by the matrix from the blue hole (Table 3). Combining the amount of water lost to or gained from the matrix with the measured change in the volume of water in the blue hole (based on its tidal amplitude) represents the total amount of water that would flow through the conduit assuming no head loss. Since there is some head loss in the conduits, the values calculated using this method are maxima.

With these assumptions, we estimate that between 0.49 and 1.2 m^3 of water exchanges with the matrix porosity during a half tidal cycle (Table 3). This volume of water represents an average of about 1% of the total change in volume of water in the blue hole. Ink Well Blue Hole has a diameter of 20 m and a maximum depth of around 8 m. Assuming a cylindrical shape, the surface area of the side is around 500 m^2, and assuming a conical shape the surface area is around 400 m^2. Assuming water flushes uniformly into matrix rocks characterized by 30% porosity, the depth of penetration would be around 6–8 mm. This value is orders of magnitude smaller than estimates of flushing into the aquifer of about 200 m on Andros Island (Whitaker and Smart, 1997b), but high permeability layers would allow water in portions of the blue hole to flush further into matrix than the average estimate. On average, however, the exchange appears to impact only a small rim around the surface of the blue hole.

5.3. Chemical effects of exchange

Exchange of water between the aquifer matrix and blue holes results in variations in chemical composition through the water column at both Ink Well Blue Hole and Mermaid Pond (Fig. 5).

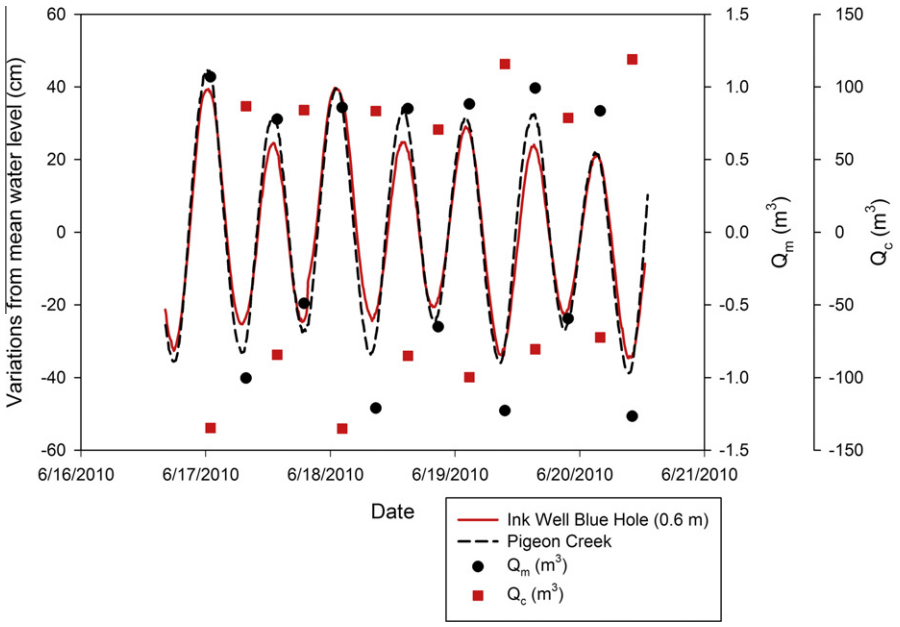

Fig. 7. (A) Variations in the elevations at Ink Well Blue Hole and Pigeon Creek around the mean elevation. The difference in the elevation is assumed to be the gradient between the ocean and Ink Well Blue Hole. At high tide Ink Well Blue Hole has lower water elevation than the ocean so the gradient is toward the blue hole and at low tide the gradient is reversed. These gradients are used to estimate exchange of water (labeled as Q) into and out of the Ink Well Blue Hole. The points represent the exchange of water into (positive) and out of Ink Well Blue Hole (negative) during the period when the water levels were either above or below the average. Q_m represents the exchange with the matrix and Q_c represent exchange through the conduit. Values of Q are given in Table 3.

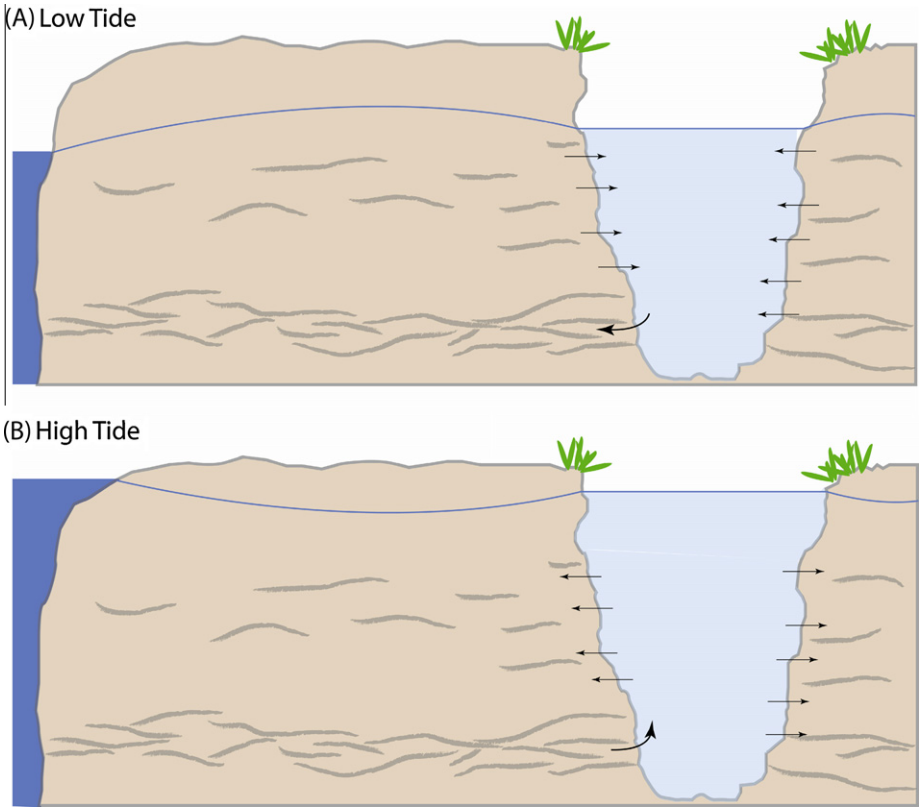

Fig. 8. Conceptual model of mixing between aquifer porosity and blue holes at (A) low tide and (B) high tide. The dark blotches within the aquifer represent zones with higher permeability than the surrounding rock that would act as preferential flow paths. The greater density of preferential flow paths with depth reflects the greater age of the strata, and thus the greater extent of their diagenetic alteration, creation of conduits and increased permeability (e.g., Vacher, 1988). This high permeability zone connects the blue hole to the ocean and allows the head in the blue hole to change more quickly than the surrounding matrix. The large arrow reflects flow through a high permeability zone between the blue hole and the ocean. The small arrows reflect the direction of slower flow between the matrix and blue hole. Vertical exaggeration is about 10 times.

Table 3
Estimates of Ink Well Blue Hole – aquifer exchange[a].

Date and time	Volume change[b] (m^3/half tidal cycle)	Matrix exchange	Conduit exchange[c]
6/17/2010 0:56	−134.7	1.07	−135.8
6/17/2010 7:46	86.7	−1.00	87.7
6/17/2010 13:46	−84.3	0.78	−85.1
6/17/2010 18:56	84.0	−0.49	84.5
6/18/2010 2:16	−135.1	0.86	−135.9
6/18/2010 8:46	83.4	−1.21	84.6
6/18/2010 14:56	−85.1	0.85	−85.9
6/18/2010 20:46	70.6	−0.65	71.3
6/19/2010 2:46	−99.7	0.88	−100.6
6/19/2010 9:36	115.7	−1.23	117.0
6/19/2010 15:26	−80.5	0.99	−81.5
6/19/2010 21:46	78.6	−0.59	79.2
6/20/2010 3:56	−72.4	0.83	−73.3
6/20/2010 10:06	118.9	−1.27	120.2

[a] Negative values represent flow out of blue hole and positive values represent flow into blue hole.
[b] Volume change represents the measured difference in the volume of water in Ink Well Blue Hole from slack water to low water (negative) or high water (positive).
[c] Conduit exchange is the total amount of water flowing to and from the blue hole including measured tidal differences and the water lost to or gained from the aquifer.

The low tide profile shows lower specific conductivity than the high tide profile at all depths in both the April and June profiles at Ink Well Blue Hole (Figs. 5A and B). This effect is clearly shown in the profile collected April 25, 2010 at a tidal stage intermediate between high and low tide when specific conductivity values are close to the low tide values to a depth of around 4 m, but are closer to the high tide values below this depth (Fig. 5A). Similarly, the profile of pH values at Ink Well Blue Hole shows different inflection points with depth between high and low tide (Fig. 6A). The elevated pH at about 4 m water depth suggests the water was buffered through reactions with the carbonate minerals. The increase in pH from low to high tide reflects flow of water into the blue hole from its sides following high tide. If similar exchange occurs between the sides of the conduits and surrounding matrix along the entire length of conduits between the blue hole and the ocean, diagenetic alteration could be further dispersed throughout the aquifer, as suggested by Whitaker and Smart (1997a).

The values of specific conductivity throughout the depth profiles also reflect mixing between the fresh water lens and seawater. The highest specific conductivity values at high tide at both Ink Well Blue Hole and Mermaid Pond are about 20,000 μS/cm lower than the value at Pigeon Creek reflecting about a 40% dilution of seawater (Fig. 5). This dilution indicates that neither blue hole penetrates completely through the halocline to pure seawater. The lower value of specific conductivity at low tide at Ink Well Blue Hole reflects a nearly 60% dilution of seawater. This difference in specific conductivity between high and low tide at the base of the profiles reflect mixing of fresh water with seawater either through the sides of the blue hole or directly into the conduit during tidal flow.

Time series measurements at different depths in Ink Well Blue Hole also reflect differential flow into the blue hole (Fig. 3A). Only the profile at 2-m depth exhibits a smoothly varying sinusoidal tidal

signal as the halocline moved past the AquaTroll during the tidal cycle. Specific conductivity recorded at the shallowest AquaTroll, at a depth of around 0.6 m, shows flattening of the profiles at low tide and at the two deepest AquaTrolls, at depths around 4 and 6 m, show flattening of the profiles at high tide. The constant salinity with time at high tide in the deepest AquaTrolls reflects its position in the deep and approximately constant salinity water with a flood tide. Similarly, the constant salinity with time at low tide in the uppermost AquaTroll reflects its position in the upper portion of the fresh water lens with ebb tide. The specific conductivity also differs between rising and falling tides for the two deepest AquaTrolls. The profiles overlap while conductivity values increase on the rising tide, but during the falling tide the drop in specific conductivity value at 4-m depth decreases earlier than the drop in specific conductivity value in the AquaTroll at 6-m depth (Fig. 3A). The similar specific conductivity values during the rising tide reflect loss of water from the blue hole to the aquifer rocks (Fig. 8), which would not change the specific conductivity of the water. The earlier decrease in the specific conductivity at 4-m depth reflects inflow of freshwater through the sides of the blue hole.

5.4. Implications for exchange

Circulation through carbonate platforms has been suggested to result from Kohout convection (Kohout, 1965), differences in the elevation head caused by oceanic circulation, buoyancy circulation from the fresh water lens, reflux driven by density differences from evaporative concentration of seawater (Whitaker and Smart, 1990). None of these mechanisms is likely to drive flow through small isolated platforms similar to Rum Cay and San Salvador Island (e.g., Martin and Moore, 2008). The specific conductivity, DO concentration and pH profiles from Mermaid Pond and Ink Well Blue Hole indicate the chemical compositions of groundwater flow in these small islands are modified by exchange processes driven by differences in hydraulic conductivity throughout the aquifer. Although this tidal pumping appears to exchange only a small fraction of water between blue holes and the surrounding matrix rocks, differences in composition of the blue hole water (e.g., Fig. 6A) suggests the exchange is important for carbonate platform diagenesis. Much alteration could be the transformation of less stable aragonite to more stable calcite (e.g., Budd, 1988). Other mineralogical transformations, such as formation of dolomite, are less likely because changes in water chemistry at these shallow depths are small and thus unlikely to overcome kinetic inhibitions to dolomite formation (e.g., Baker and Kastner, 1981).

Previous work on blue holes and cenotes on large carbonate platforms have found stable haloclines that affect alteration of the carbonate minerals through redox alteration of organic carbon trapped on the pycnoclines (Stoessell, 1995; Beddows et al., 2007). Even in systems with stable pycnoclines, tidal pumping causes the exchange of water undersaturated with respect to carbonate minerals through oxidation of organic carbon in the blue holes. Such focusing could cause deeper penetration of undersaturated water into the matrix than the 6–8 mm estimated above for Ink Well Blue Hole. This undersaturated water would dissolve aquifer rocks along preferential flow paths and within matrix porosity. Horizontal flow occurs over long distances in integrated conduit systems in the Yucatan Peninsula that have aggregate lengths up to hundreds of kilometers (Smart et al., 2006). This flow will be influenced by tidal pumping and mixing with seawater since coastal springs in the Yucatan are known to have tidally driven ebb and flood cycles, although it is not known how far inland these flow reversals extend (Beddows, 2003). Assuming tidal exchange between blue holes, conduits and matrix porosity occurs in the Yucatan, similar dissolution reactions should also be important to the diagenetic alteration of large platforms.

To our knowledge, no previous work has estimated how haloclines evolve through a tidal cycle in carbonate platforms. Even in large platforms such as the Yucatan, exchange between the aquifer matrix and the water column may be sufficient to influence diagenetic alteration of the platform. Bottrell et al. (1990) suggested that eddy diffusion was sufficient to drive sulfur reactions in the water column and alter pH sufficiently for carbonate dissolution reactions. Our work suggests that this exchange may also be influenced by advective exchange of blue hole and aquifer water, as well as diffusive processes in the water column. Exchange between the water column in blue holes and the aquifer matrix could influence the diagenetic evolution of these platforms. Large fresh water lenses and long distances from the coast on large platforms will dampen the tidal mixing, but tidal pumping into and out of conduits and coupled exchange with the matrix porosity should be important factors in the alteration of the platforms nearer to the coast similar to the exchange observed on San Salvador Island and Rum Cay. Detailed measurements of chemical profiles of components involved in carbonate mineral reactions will be needed through tidal cycles, either within conduits or at blue holes distributed throughout the platform to test this hypothesis.

6. Conclusions

Tidal pumping of conduits in small carbonate islands provides a mechanism to drive the exchange of surface water with water in matrix porosity. This mixing can be observed in variations in composition of the water column of blue holes through a tidal cycle. At sites observed in this study, only about 1% of the total tidal change in volume of water in the blue hole exchanged with water within the aquifer rocks and penetrated into the matrix to average depths of 6–8 mm, although focusing could cause deeper penetration. Although the volume of water exchanged through tidal cycles is small relative to the total volume of water in the blue holes, specific conductivity of water differed by up to 25% between high and low tide. Since exchange occurs twice daily, its time-integrated impact on diagenetic alteration of the aquifer could be large. Tidally driven exchange of surface water and aquifer water could impact dissolution patterns on carbonate platforms by supplying organic carbon to the matrix where subsequent microbial oxidation would increase matrix porosity, but since tides are dampened with distance inland, this dissolution should decrease away from the coast.

Acknowledgments

We gratefully acknowledge field and logistical support provided by Tom Rothfus and the staff at the Gerace Research Centre, San Salvador Island, and by Josie Harding on Rum Cay. We thank the Bahamas Environment, Science and Technology Commission for permission to conduct this research. We thank David Budd and an anonymous reviewer for their helpful reviews. Acknowledgment is made to the Donors of the American Chemical Society Petroleum Research Fund for support of this research. Additional support was provided to JG in the form of a National Science Foundation Graduate Fellowship and an NSF EAR Postdoctoral Research Fellowship (#0946767).

References

Ayers, J.F., Vacher, H.L., 1986. Hydrogeology of an atoll island: a conceptual model from detailed study of a Micronesian example. Ground Water 24, 185–198.
Baker, P.A., Kastner, M., 1981. Contraints on the formation of sedimentary dolomite. Science 213, 214–216.
Beach, D.K., Ginsburg, R.N., 1980. Facies succession of pliocene–pleistocene carbonates, northwestern Great Bahama Bank. Am. Assoc. Petrol. Geol. Bull. 64, 1634–1642.
Beddows, P.A., 2003. Cave hydrology of the Caribbean Yucatan coast. Assoc. Mex. Cave Stud. Bull. 11, 96.

Beddows, P.A., Smart, P.L., Whitaker, F.F., Smith, S.L., 2007. Decoupled fresh–saline groundwater circulation of a coastal carbonate aquifer: spatial patterns of temperature and specific electrical conductivity. J. Hydrol. 346 (1–2), 18–32.
Bottrell, S.H., Smart, P.L., Whitaker, F.F., Raiswell, R., 1990. Geochemistry and isotope systematics of sulphur in the mixing zone of Bahamian blue holes. Appl. Geochem. 6, 97–103.
Budd, D.A., 1988. Aragonite-to-calcite transformation during fresh-water diagenesis of carbonates: insights from pore-water chemistry. Geol. Soc. Am. Bull. 100, 1260–1270.
Cant, R.V., Weech, P.S., 1986. A review of the factors affecting the development of Ghyben–Hertzberg lenses in the Bahamas. J. Hydrol. 84, 333–343.
Carew, J.L., Mylroie, J.E., 1995. Depositional model and stratigraphy for the quaternary geology of the Bahama islands. Geol. Soc. Am. 1, 5–32.
Davis, R.L., Johnson, J., C.R., 1989. Karst Hydrology of San Salvador. In: Mylroie, J.E. (Ed.). In: Proceedings, Fourth Symposium on the Geology of the Bahamas. Bahamian Field Station, San Salvador Island, Bahamas, pp. 118–135.
Ferris, J.G., 1951. Cyclic fluctuations of water level as a basis for determining aquifer transmissibility. Assem. Gen. Bruxelles, Assoc. Int. Hydrol. Sci. 2, 149–155.
Ford, D., Williams, P., 2007. Karst Hydrogeology and Geomorphology. John Wiley and Sons, West Sussex, p. 562.
Gulley, J., Martin, J.B., Screaton, E.J., Moore, P.J., 2011. River reversals into karst springs: a model for cave enlargement in eogenetic karst aquifers. Geol. Soc. Am. Bull. 123, 467.
Kohout, F.A., 1965. A hypothesis concerning the cyclic flow of salt water related to geothermal heating in the Florida aquifer. NY Acad. Sci. Trans. 28, 249–271.
Little, B.G., Buckley, D.K., Jefferiss, A., Stark, J., Young, R.N., 1973. Land resources of the commonwealth of the Bahamas, 4, Andros island. Ministry of Overseas Development, Surbiton, England.
Martin, J.B., Dean, R.W., 2001. Exchange of water between conduits and matrix in the Floridan aquifer. Chem. Geol. 179, 145–165.
Martin, J.B., Gulley, J., 2010. Distribution of fresh water on Rum Cay and implications for generation of secondary porosity. In: Siewers, F.E., Martin, J.B. (Eds.), Proceedings of the 14th Symposium on the Geology of the Bahamas and Other Carbonate Regions. Gerace Research Centre, San Salvador Island, Bahamas, pp. 140–149.
Martin, J.B., Moore, P.J., 2008. Sr concentrations and isotope ratios as tracers of ground-water circulation in carbonate platforms: examples from San Salvador island and long island, Bahamas. Chem. Geol. 249, 52–65.
McGee, D.K., Wynn, J.G., Onac, B.P., Harries, P.J., Rothfus, E.A., 2010. Tracing groundwater geochemistry using $d^{13}C$ on San Salvador island (southeastern Bahamas): implications for carbonate island hydrogeology and dissolution. Carbonates Evaporites, doi: 10.1007/s13146-010-0013-6.
Melim, L.A., Westphal, H., Swart, P.K., Eberli, G.P., Munnecke, A., 2002. Questioning carbonate diagenetic paradigms: evidence from the Neogene of the Bahamas. Mar. Geol. 185 (1–2), 27–53.
Mitchell, S.W., 1987. Surficial geology of Rum Cay, Bahama islands. In: Curran, H.A. (Ed.). In: Proceedings of the Third Symposium on the Geology of the Bahamas. CCFL Bahamian Field Station, Fort Lauderdale, Florida, pp. 231–241.
Moore, P.J., 2009. Controls on the Generation of Secondary Porosity in Eogenetic Karst: Examples from San Salvador Island, Bahamas and North-Central Florida. University of Florida, Gainesville, FL, p. 140.
Moore, P.J., Martin, J.B., Screaton, E.J., 2009. Geochemical and statistical evidence of recharge, mixing, and controls on spring discharge in an eogenetic karst aquifer. J. Hydrol. 376 (3–4), 443–455.
Moore, P.J., Martin, J.B., Screaton, E.J., Neuhoff, P.S., 2010. Conduit enlargement in an eogenetic karst aquifer. J. Hydrol. 393, 143–155.
Mylroie, J.E., Carew, J.L., 1990. The flank margin model for dissolution cave development in carbonate platforms. Earth Surf. Proc. Land. 15, 413–424.
Mylroie, J.E., Carew, J.L., 1995. Karst Development on Carbonate Islands. In: Budd, D.A., Harris, P.M., Saller, A. (Eds.), Unconformities and Porosity in Carbonate Strata. American Association of Petroleum Geologists, pp. 55–76.
Mylroie, J.E., Carew, J.L., Moore, A.I., 1995. Blue holes: definition and genesis. Carbonates Evaporites 10, 225–233.
Oberdorfer, J., Hogan, P., Buddemeier, R., 1990. Atoll island hydrogeology: flow and freshwater occurrence in a tidally dominated system. J. Hydrol. 120, 327–340.
Perry, E., Marin, L., McClain, J., Velazquez, G., 1995. Ring of cenotes (sinkholes) northwest Yucatan, Mexico: its hydrogeologic characteristics and possible association with the chicxulub impact crater. Geology 23, 17–20.
Runnells, D.D., 1969. Diagenesis, chemical sediments, and the mixing of natural waters. J. Sediment. Petrol. 39, 1188–1201.
Schwabe, S., Herbert, R.A., 2004. Black holes of the Bahamas: what they are and why they are black. Quatern. Int. 121 (1), 3–11.
Sealey, N.E., 2006. Bahamian LANDSCAPES; an introduction to the physical geography of the Bahamas. Macmillan Publishers, Oxford, p. 174.
Smart, P.L. et al., 2006. Cave Development on the Caribbean Coast of the Yucatan Peninsula, Quintana Roo, Mexico. In: Harmon, R.S., Wicks, C. (Eds.), Perspectives on Karst Geomorphology, Hydrology, and Geochemistry – A Tribute Volume to Derek C. Ford and William B. White. Geological Society of America, Denver, CO, pp. 105–128.
Stoessell, R., 1995. Dampening of transverse dispersion in the halocline in karst limestone int he northeastern Yucatan Peninsula. Ground Water 33, 366–371.
Stoessell, R.K., Coke, J.G., Easley, D.H., 2002. Localized thermal anomalies in haloclines of coastal Yucatan sinkholes. Ground Water 40, 416–424.
Stringfield, V.T., LeGrand, H.E., 1971. Effects of karst features on circulation of water in carbonate rocks in coastal areas. J. Hydrol. 14 (2), 139–157.
Townley, L.R., 1995. The response of aquifers to periodic forcing. Adv. Water Resour. 18, 125–146.
Vacher, H.L., 1988. Dupuit–Ghyben–Herzberg analysis of strip-island lenses. Geol. Soc. Am. Bull. 100, 580–591.
Vacher, H.L., Mylroie, J.E., 2002. Eogenetic karst from the perspective of an equivalent porous medium. Carbonates Evaporites 17, 182–196.
Vacher, H.L., Quinn, T.M., 1997. Geology and Hydrogeology of Carbonate Islands. Elsevier, Amsterdam, p. 948.
Vacher, H.L., Wallis, T.N., 1992. Comparative hydrogeology of fresh-water lenses of Bermuda and Great Exumas island, Bahamas. Ground Water 30, 15–20.
Whitaker, F.F., Smart, P.L., 1990. Active circulation of saline ground waters in carbonate platforms: evidence from the Great Bahama Bank. Geology 18 (3), 200–204.
Whitaker, F.F., Smart, P.L., 1997a. Groundwater circulation and geochemistry of a karstified bank-marginal fracture system, south Andros island, Bahamas. J. Hydrol. 197 (1–4), 293–315.
Whitaker, F.F., Smart, P.L., 1997b. Hydrogeology of the Bahamian Archipelago. In: Vacher, H.L., Quinn, T. (Eds.), Geology and Hydrogeology of Carbonate Islands. Developments in Sedimentology 54. Elsevier Science B.V., Amsterdam, pp. 183–216.
Whitaker, F.F., Smart, P.L., 2007a. Geochemistry of meteoric diagenesis in carbonate islands of the northern Bahamas: 1. Evidence from field studies. Hydrol. Process. 21, 949–966.
Whitaker, F.F., Smart, P.L., 2007b. Geochemistry of meteoric diagenesis in carbonate islands of the northern Bahamas: 2. Geochemical modelling and budgeting of diagenesis. Hydrol. Process. 21, 967–982.
Wigley, T.M.L., Plummer, L.N., 1976. Mixing of carbonate waters. Geochim. Cosmochim. Acta 40 (9), 989–995.